JZUS

Residual intensity modulation in resonator fiber optic gyros with sinusoidal wave phase modulation[*]

Di-qing YING[†], Qiang LI, Hui-lian MA, Zhong-he JIN

(*Micro-Satellite Research Center, Zhejiang University, Hangzhou 310027, China*)

[†]E-mail: dqying@zju.edu.cn

Abstract: We present how residual intensity modulation (RIM) affects the performance of a resonator fiber optic gyro (R-FOG) through a sinusoidal wave phase modulation technique. The expression for the R-FOG system's demodulation curve under RIM is obtained. Through numerical simulation with different RIM coefficients and modulation frequencies, we find that a zero deviation is induced by the RIM effect on the demodulation curve, and this zero deviation varies with the RIM coefficient and modulation frequency. The expression for the system error due to this zero deviation is derived. Simulation results show that the RIM-induced error varies with the RIM coefficient and modulation frequency. There also exists optimum values for the RIM coefficient and modulation frequency to totally eliminate the RIM-induced error, and the error increases as the RIM coefficient or modulation frequency deviates from its optimum value; however, in practical situations, these two parameters would not be exactly fixed but fluctuate from their respective optimum values, and a large system error is induced even if there exists a very small deviation of these two critical parameters from their optimum values. Simulation results indicate that the RIM-induced error should be considered when designing and evaluating an R-FOG system.

1 Introduction

Based on the Sagnac effect, the resonator fiber optic gyro (R-FOG) has potential to be used as a high accuracy inertial rotation sensor (Shupe, 1981; Meyer *et al.*, 1983; Chow *et al.*, 1985; Malvern, 1992; Ying *et al.*, 2008a). It has been theoretically proven that an R-FOG has similar shot-noise-limited performance to an interferometric fiber optic gyro (I-FOG) but requires a shorter length of fiber (Shupe, 1981); therefore, it is meaningful to study and develop the R-FOG for its advantages in further reducing gyro size and cost. The LiNbO$_3$ phase modulator is an essential signal processing component in the R-FOG system (Hotate and Harumoto, 1997; Hotate and Hayashi,

1999; Zhang *et al.*, 2005; 2006a), and it has many advantages such as small size and large modulation bandwidth (Savatinova *et al.*, 1996; Zhang and Wang, 1996). Nevertheless, when the phase modulator is driven by a voltage phase modulation signal, the residual intensity modulation (RIM) effect will also be induced (Jaatinen *et al.*, 2009; Sathian and Jaatinen, 2012), which would affect the performance of the gyro system. The RIM effect in I-FOG has been looked into by many researchers. Wang and Zhang (1995) studied the RIM effect on sideband suppression, and proposed some methods to decrease this effect. Wang and Sheng (2007) pointed out that the RIM can generate signal bias or increase noise. Hu (2008) and Li *et al.* (2009) found that the RIM effect would reduce the stability of I-FOG's scalar factor.

To the best of our knowledge, however, there has been no in-depth analysis of the RIM effect in an R-FOG. In this paper, we analyze in detail how the

---

RIM effect affects an R-FOG with the sinusoidal wave phase modulation technique (Zhang *et al*., 2005; 2006a). The characteristics of R-FOG's demodulation curve play an important role in system performance (Ma *et al*., 2004; Zhang *et al*., 2005; 2006a; Ying *et al*., 2008a; 2008b). In previous research (Ying *et al*., 2010), through exploring the zero-point characteristics of the demodulation curve, how the Kerr effect influences R-FOG performance has been discussed. Here, we use a similar method to discuss the RIM effect (Ying *et al*., 2010). Using the Bessel function and the method of optic field overlapping, we obtain the expression for the demodulation curve under the RIM effect. By numerical simulation, we discuss the demodulation characteristics with different RIM coefficients and modulation frequencies, and analyze the zero deviation induced by the RIM effect. Through studying the zero deviation for two counter propagating beams, we present the expression for the RIM-induced error. By simulation, we discuss how the RIM-induced error varies with the RIM coefficient and modulation frequency.

2 Theoretical formulation

Fig. 1 illustrates the system configuration of the R-FOG system with sinusoidal wave phase modulation (Ma *et al*., 2012). All the fibers are polarization preserving in the system. The central wavelength and line width of the laser are 1550 nm and 5 kHz, respectively. The laser is equally divided into two beams by a coupler C0 and each beam is sinusoidal wave phase modulated by LiNbO$_3$ phase modulators PM1 and PM2, respectively. Then, these two beams are injected into the fiber ring resonator (FRR) in clockwise (CW) and counter clockwise (CCW) directions. The CW and CCW beams output from the FRR are sensed by InGaAs PIN photodetectors PD1 and PD2, respectively. The CCW signal is demodulated by the digital lock-in-amplifier LIA2, and the demodulation signal is used to lock the central frequency of the laser to the CCW resonance of the FRR through the servo controller. The CW signal is demodulated by the digital lock-in-amplifier LIA1 and the demodulated signal is proportional to the rotation rate (Ma *et al*., 2012).
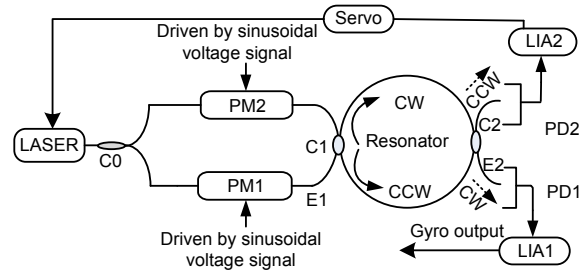

Fig. 1 System configuration of the R-FOG with sinusoidal phase modulation
CW: clockwise; CCW: counter clockwise; C0−C2: couplers; PD1, PD2: photodetectors; PM1, PM2: phase modulators

The output electric field of the laser can be written as

$$E_{\mathrm{LASER}}(t) = E_0 \exp[\mathrm{j}(2\pi f_0 t + \phi_0)], \qquad (1)$$

where E_0 is the amplitude of the electric field of the laser light, f_0 is the central frequency of the laser, and ϕ_0 is the initial phase. Due to the RIM effect, when the laser beam goes through the phase modulator driven by the sinusoidal voltage signal, it will also be intensity modulated in addition to being phase modulated; therefore, the electric field after PM1 can be written as (Zhang *et al*., 2005; Hu, 2008; Ying *et al*., 2008a)

$$
\begin{aligned}
E_{\mathrm{M\_CW}}(t) = {} & E_0 \sqrt{1 + \varepsilon_1 V_1 \sin(2\pi F_{\mathrm{CW}} t)} \\
& \cdot \sqrt{k_{\mathrm{C0}}(1 - \alpha_{\mathrm{C0}})(1 - \alpha_{\mathrm{PM1}})} \qquad (2) \\
& \cdot \exp\{\mathrm{j}[2\pi f_0 t + \phi_0 + M \sin(2\pi F_{\mathrm{CW}} t)]\},
\end{aligned}
$$

where ε_1 is the RIM coefficient, k_{C0} and α_{C0} are the intensity coupling coefficient and fractional intensity loss of coupler C0, respectively, α_{PM1} is the fractional insertion loss of PM1, $M = \pi V_1 / V_\pi$ is the phase modulation index, V_1 is the amplitude of the modulation signal, and V_π is the half-wave voltage of PM1. To suppress the carrier component, M is set as 2.405 rad in this study (Iwatsuki *et al*., 1984; Ying *et al*., 2008a; Jin *et al*., 2012). Using the Bessel function, Eq. (2) can be expanded as (Zhang *et al*., 2005)

$$
\begin{aligned}
E_{\mathrm{M\_CW}}(t) = {} & E_0 \sqrt{1 + \varepsilon_1 V_1 \sin(2\pi F_{\mathrm{CW}} t)} \\
& \cdot \sqrt{k_{\mathrm{C0}}(1 - \alpha_{\mathrm{C0}})(1 - \alpha_{\mathrm{PM1}})} \qquad (3) \\
& \cdot \sum_{n=-\infty}^{\infty} \mathrm{J}_n(M) \exp[\mathrm{j}(2\pi f_n t + \phi_0)],
\end{aligned}
$$

where $f_n=f_0+nF_{\text{CW}}$, n is an integer, and $J_n(M)$ is the Bessel function. Using the field overlapping method (Ma *et al*., 2003; 2004; Ying *et al*., 2008a), the output field at E2 in Fig. 1 can be written as

$$E_{\text{O\_CW}}(t) = E_0 \sqrt{1 + \varepsilon_1 V_1 \sin(2\pi F_{\text{CW}} t)}$$
$$\cdot \sqrt{k_{\text{C0}}(1-\alpha_{\text{C0}})(1-\alpha_{\text{PM1}})} \qquad (4a)$$
$$\cdot \sum_{n=-\infty}^{\infty} J_n(M) \exp[j(2\pi f_n t + \phi_0)]h_n \exp(j\phi_n),$$

where

$$h_n = QR\sqrt{\dfrac{1}{(1-TR^2)^2 + 4TR^2 \sin^2\left[\dfrac{\pi(\Delta f_{\text{CW}} + nF_{\text{CW}})}{\text{FSR}}\right]}}, \qquad (4b)$$

$$\phi_n = -\dfrac{\pi f_n}{\text{FSR}} - \arctan\left\{\dfrac{TR^2 \sin\left[2\pi\left(\dfrac{\Delta f_{\text{CW}} + nF_{\text{CW}}}{\text{FSR}}\right)\right]}{1 - TR^2 \cos\left[2\pi\left(\dfrac{\Delta f_{\text{CW}} + nF_{\text{CW}}}{\text{FSR}}\right)\right]}\right\}, \qquad (4c)$$

$$T = \sqrt{1-k_{\text{C1}}}\sqrt{1-k_{\text{C2}}}\sqrt{1-\alpha_{\text{C1}}}\sqrt{1-\alpha_{\text{C2}}}, \qquad (4d)$$

$$Q = \sqrt{k_{\text{C1}}k_{\text{C2}}}\sqrt{1-\alpha_{\text{C1}}}\sqrt{1-\alpha_{\text{C2}}}, \qquad (4e)$$

$$R = \sqrt{1-\alpha_{L/2}}, \qquad (4f)$$

where k_{C1} and k_{C2} are the intensity coupling coefficients of couplers C1 and C2 respectively, α_{C1} and α_{C2} are the fractional insertion losses of couplers C1 and C2 respectively, $\alpha_{L/2}$ is the fractional intensity loss for semi-loop of the FRR, $f_{\text{CW}}=f_0-f_{\text{R\_CW}}$ is the resonance deviation, $f_{\text{R\_CW}}$ is the resonance frequency of the FRR in the CW direction, $\text{FSR}=c/(n_r L)$ is the free spectral range, L is the length of the FRR, n_r is the refractive index of the fiber, and c is the light velocity in the vacuum. Eqs. (4b) and (4c) represent the amplitude and phase of the FRR's transfer function in the CW direction, respectively.

According to Eq. (4), the output signal of photo-detector PD1 can be written as

$$V_{\text{PD\_CW}} = G_1 I_0 P_1 [1 + \varepsilon_1 V_1 \sin(2\pi F_{\text{CW}} t)]$$
$$\cdot \sum_{n=-\infty}^{\infty}\sum_{n'=-\infty}^{\infty} \{J_n(M) J_{n'}(M) \exp[j(n-n')2\pi F_{\text{CW}} t] \qquad (5)$$
$$\cdot h_n h_{n'} \exp[j(\phi_n - \phi_{n'})]\},$$

where $G_1=k_{\text{C0}}(1-\alpha_{\text{C0}})(1-\alpha_{\text{PM1}})$, I_0 is the output intensity of the laser, and P_1 is the photoelectric conversion factor of PD1. After demodulation with respect to the first harmonic and using a band-pass filter, all the terms in Eq. (5) are eliminated except those satisfying the condition $n'=n\pm1$. Then the demodulation signal output from LIA1 can be written as (Carroll *et al*., 1987; Zhang *et al*., 2005)

$$V_{\text{d\_CW}} = G_1 I_0 P_1 A_{\text{D1}}\left[-\sum_{n=-\infty}^{\infty} J_n J_{n+1} h_n h_{n+1} \sin(\phi_{n+1} - \phi_n)\right.$$
$$\left. + \varepsilon_1 V_1 \sum_{n=-\infty}^{\infty} J_n J_n h_n h_n - \dfrac{\varepsilon_1 V_1}{2}\sum_{n=-\infty}^{\infty} J_n J_{n+2} h_n h_{n+2} \cos(\phi_{n+2} - \phi_n)\right], \qquad (6)$$

where A_{D1} is the gain of the lock-in-amplifier LIA1. Similarly, the demodulation signal output from LIA2 can be written as

$$V_{\text{d\_CCW}} = G_2 I_0 P_2 A_{\text{D2}}[-\sum_{n=-\infty}^{\infty} J_n J_{n+1} h'_n h'_{n+1} \sin(\phi'_{n+1} - \phi'_n)$$
$$+ \varepsilon_2 V_2 \sum_{n=-\infty}^{\infty} J_n J_n h'_n h'_n$$
$$- \dfrac{\varepsilon_2 V_2}{2}\sum_{n=-\infty}^{\infty} J_n J_{n+2} h'_n h'_{n+2} \cos(\phi'_{n+2} - \phi'_n)], \qquad (7)$$

where $G_2=k_{\text{C0}}(1-\alpha_{\text{C0}})(1-\alpha_{\text{PM2}})$, P_2 is the photoelectric conversion factor of PD2, A_{D2} is the gain of lock-in-amplifier LIA2, ε_2 is the residual intensity modulation coefficient of PM2, h'_n and ϕ'_n are the amplitude and phase of the FRR's transfer function in the CCW direction respectively, which have the same forms as h_n and ϕ_n in the CW direction respectively, V_2 is the amplitude of the sinusoidal modulation signal $V_2\sin(2\pi F_{\text{CCW}} t)$ used to drive PM2, and the frequency of the modulation signal is F_{CCW}. According to Eqs. (6) and (7), the demodulation signals $V_{\text{d\_CW}}$ and $V_{\text{d\_CCW}}$ are functions of the RIM coefficients ε_1 and ε_2, which means the RIM would affect the performance of the R-FOG system.

3 Simulation and discussion

Based on Eqs. (6) and (7), we conduct numerical simulation on the performance of R-FOG under the RIM effect. Fig. 2 shows the calculated demodulation

curve for the CW loop near $\Delta f_{CW}=0$. The modulation frequency is fixed at $F_{CW}=101$ kHz, while the RIM coefficient takes three different values of $\varepsilon_1=0$, 0.0003 and 0.0005 V^{-1}. The fiber length L of the FRR is 15 m, the refractive index n_r of the fiber is 1.455, the fractional intensity losses α_{C0}, α_{C1}, and α_{C2} for couplers C0, C1, and C2 respectively are all 0.0228, the fractional insertion loss α_{PM1} of PM1 is 0.5, the intensity coupling coefficient k_{C0} of coupler C0 is 0.5, the intensity coupling coefficients k_{C1} and k_{C2} for couplers C1 and C2 respectively are both set to 0.03, the fractional intensity loss $\alpha_{L/2}$ for the semi-loop of the FRR is 0.00035, the photoelectric conversion factor P_1 of PD2 is 0.5 V/mW, the output intensity I_0 of the laser is assumed to be 1 mW, and the gain A_{D1} of lock-in-amplifier LIA1 is 1. Since the half-wave voltage V_π of PM1 is 9.92 V in our R-FOG system, the amplitude V_1 of the modulation signal is set as 7.6 V, so that the phase modulation index M reaches its optimum value 2.405 rad. As can be seen from Fig. 2, when ε_1 is 0, the demodulation output V_{d_CW} is equal to zero for $\Delta f_{CW}=0$, indicating that no error occurs when RIM is not considered. However, when ε_1 is 0.0003 or 0.0005 V^{-1}, the value of Δf_{CW} at the zero-crossing point would not be zero but is equal to a zero deviation Δf_{d_CW} (Fig. 2), and this RIM-induced zero deviation would cause an error in the R-FOG system, which will be specifically discussed in the following.
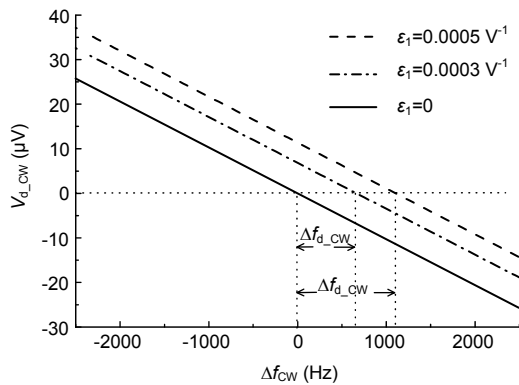

Fig. 2 Demodulation curve for CW loop with different ε_1 (F_{CW} is fixed at 101 kHz)

Fig. 3 shows the demodulation curve of the CW loop when ε_1 is fixed at 0.0005 V^{-1} with $F_{CW}=96$, 101, and 106 kHz. Other parameters are the same as

aforementioned. As can be seen from Fig. 3, under the RIM effect, the value of Δf_{d_CW} varies with different values of F_{CW}. Therefore, the error induced by the RIM effect would be related to the modulation frequency.
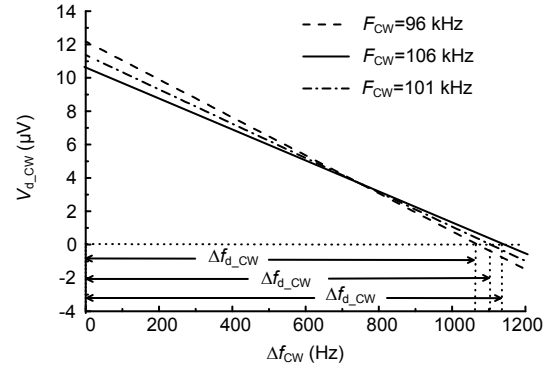

Fig. 3 Demodulation curve with different F_{CW} (ε_1 is fixed at 0.0005 V^{-1})

Similarly, the zero deviation Δf_{d_CCW} of the demodulation curve would also be induced for the CCW loop when the RIM effect is considered, and it also varies with the modulation frequency and RIM coefficient. To further discuss how the RIM effect influences the R-FOG system performance, we derive the expression for the system error induced by the RIM effect, which is a function of the modulation frequency and RIM coefficient. According to Eqs. (6) and (7), the zero deviations Δf_{d_CW} and Δf_{d_CCW} can be obtained by solving (Ying et al., 2008b; 2010)

$$V_{out\_CW}(\Delta f_{CW})|_{\Delta f_{CW}=\Delta f_{d\_CW}}=0, \qquad (8)$$

$$V_{out\_CCW}(\Delta f_{CCW})|_{\Delta f_{CCW}=\Delta f_{d\_CCW}}=0, \qquad (9)$$

where $f_{CCW}=f_0-f_{R\_CCW}$ is the resonance deviation for the CCW loop, and f_{R_CCW} is the resonance frequency. The CCW loop in our R-FOG system is a closed loop, which means that the operating point is always fixed at the resonance; therefore, f_0 and f_{d_CCW} satisfy (Iwatsuki et al., 1986; Zhang et al., 2006b; Ying et al., 2010)

$$f_0 = f_{R\_CCW} + \Delta f_{d\_CCW}. \qquad (10)$$

For the CW loop, which is an open loop in our system (Ma et al., 2012), when the demodulation output is

zero, f_0 and f_{d_CW} satisfy

$$f_0 = f_{R\_CW} + \Delta f_{d\_CW}. \qquad (11)$$

Subtracting Eq. (11) from Eq. (10), we can obtain the resonance frequency difference between CW and CCW loops when the gyro output is zero:

$$\Delta f_e = f_{R\_CW} - f_{R\_CCW} = \Delta f_{d\_CCW} - \Delta f_{d\_CW}. \qquad (12)$$

Hence, according to the Sagnac effect, the system error introduced by RIM can be expressed by (Meyer *et al.*, 1983; Lefevre, 1993)

$$\Omega_e = \frac{n_r \lambda}{D} \Delta f_e, \qquad (13)$$

where D is the diameter of the FRR, and λ is the central wavelength of the laser.

Fig. 4 shows the calculated system error due to the RIM effect as a function of ε_2 with ε_1=0.0004, 0.0005, and 0.0006 V^{-1}. The modulation frequencies F_{CW} and F_{CCW}, which would be different from each other in suppressing the backscattering noise (Iwatsuki *et al.*, 1984; 1986; Hotate and Harumoto, 1997; Hotate and Hayashi, 1999; Jin *et al.*, 2012), are set as 101 and 103 kHz, respectively. The fractional insertion loss of PM2 and the photoelectric conversion factor of PD2 are assumed to be the same as their counterparts in the CW loop. The diameter D of the FRR is 0.14 m, and the gain A_{D2} of lock-in-amplifier LIA2 is 1. As can be seen from Fig. 4, for a particular ε_1 there exists an optimum value of ε_2 that leads to Ω_e=0, which indicates that the RIM-induced error could be completely removed as long as the RIM coefficient of the phase modulator is fixed at its optimum value. However, on the one hand, the value of the RIM coefficient cannot be easily controlled during the production process of the phase modulator; on the other hand, the RIM coefficient fluctuates due to environmental factors when the phase modulator is used in the R-FOG system (Hu, 2008). Because of this effect, the RIM coefficient generally deviates from its optimum value, which would inevitably cause an R-FOG system error. Taking ε_1=0.0005 V^{-1} as an example, the optimum value of ε_2 is about

0.00049 V^{-1}, and when ε_2 deviates from its optimum value by about 0.00001 V^{-1}, the RIM-induced error is about 55.14 deg/h.
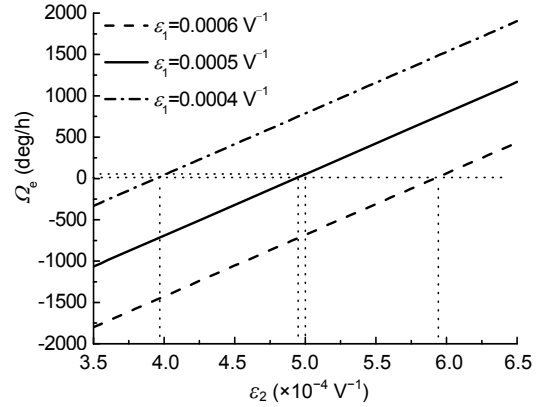

Fig. 4 Relationship between RIM-induced error Ω_e and RIM coefficient ε_2 with different values of ε_1

Fig. 5 shows the calculated system error due to the RIM effect as a function of F_{CCW} with F_{CW}=96, 101, and 106 kHz. In the practical situation, since it is not easy to control the two RIM coefficients to be exactly the same due to the uncertainty of these two coefficients, as mentioned above, we set ε_1 and ε_2 to be 0.0005 and 0.00048 V^{-1}, respectively. As can be seen from Fig. 5, for a particular F_{CW} there exists an optimum value of F_{CCW} that leads to Ω_e=0, and the RIM-induced error increases as F_{CCW} deviates from its optimum value. Thus, we could choose the optimum modulation frequency for the R-FOG system to completely remove the RIM-induced error. However, the modulation frequency is also closely related to other R-FOG system factors, such as the Kerr noise (Ying *et al.*, 2010), backscattering noise (Iwatsuki *et al.*, 1984; Jin *et al.*, 2012), and slope of the demodulation curve (Zhang *et al.*, 2005), which have their own different optimum modulation frequencies. All these factors should be considered when we design the modulation frequency; therefore, in practical situations, the RIM-induced error would not be totally eliminated for the chosen modulation frequency which is generally different from its optimum value to suppress the RIM error. Taking F_{CW}=101 kHz as an example, the RIM-induced error would be about 253.4 deg/h when F_{CCW} equals 105 kHz, which deviates from its optimum value by about 10.2 kHz.
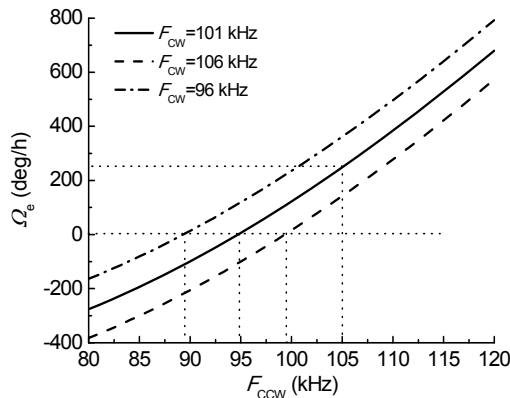
Fig. 5 Relationship between RIM-induced error Ω_e and F_{CCW} with different F_{CW}

4 Conclusions

Through theoretical analysis and simulation, we have studied how the phase modulator's RIM effect influences the performance of the R-FOG system with sinusoidal wave phase modulation. It is found that under the RIM effect, a zero deviation would be induced on the demodulation curve, and this zero deviation varies with the RIM coefficient and modulation frequency. This zero deviation would induce an error in the R-FOG system. It is concluded that the RIM-induced error is a function of the RIM coefficient for the two counter propagating beams, and there exist optimum values for the RIM coefficient to totally eliminate the RIM-induced error. When the RIM coefficient deviates from its optimum value, the system error increases, and for a 15 m FRR, simulation results indicate that a 55.14 deg/h system error would be induced even if the RIM coefficient deviates from the optimum value by only 0.00001 V^{-1}. In addition, it is found that the RIM-induced error is related to the modulation frequency for the two counter propagating beams, and that the RIM-induced error could be completely suppressed by choosing a group of optimum modulation frequencies. Nevertheless, the modulation frequencies chosen in practical situations would generally be different from the optimum value to minimize the RIM-induced error. It has been proven that the system error increases as the modulation frequency deviates from the optimum value, and simulation results show that a 253.4 deg/h

RIM-induced error would be induced if the modulation frequency deviates from the optimum value by 10.2 kHz, and this system error together with that caused by the RIM coefficient deviating from the optimum value should be counted for a medium accuracy R-FOG. These results are useful in optimizing and evaluating the performance of the R-FOG system.

References

Carroll, R., Coccoli, C.D., Cardarelli, D., *et al.*, 1987. The passive resonator fiber optic gyro and comparison to the interferometer fiber gyro. Fiber Optic Gyros: 10th Anniversary Conf. Int. Society for Optics and Photonics, p.169-177.

Chow, W.W., Gea-Banaciloche, J., Pedrotti, L.M., *et al.*, 1985. The ring laser gyro. *Rev. Mod. Phys.*, **57**(1):61-103. [doi:10.1103/RevModPhys.57.61]

Hotate, K., Harumoto, M., 1997. Resonator fiber optic gyro using digital serrodyne modulation. *J. Lightw. Technol.*, **15**(3):466-473. [doi:10.1109/50.557562]

Hotate, K., Hayashi, G., 1999. Resonator fiber optic gyro using digital serrodyne modulation-method to reduce the noise induced by the backscattering and closed-loop operation using digital signal processing. *SPIE*, **3746**:104-107.

Hu, Z., 2008. Effects of residual intensity modulation of Y-waveguide modulator on interferometric fiber optic gyroscope and elimination method. *Chin. J. Lasers*, **35**(12):1924-1929 (in Chinese). [doi:10.3788/CJL2008 3512.1924]

Iwatsuki, K., Hotate, K., Higashiguchi, M., 1984. Effect of Rayleigh backscattering in an optical passive ring-resonator gyro. *Appl. Opt.*, **23**(21):3916-3924. [doi:10. 1364/AO.23.003916]

Iwatsuki, K., Hotate, K., Higashiguchi, M., 1986. Kerr effect in an optical passive ring-resonator gyro. *J. Lightw. Technol.*, **4**(6):645-651. [doi:10.109/JLT.1986.1074770]

Jaatinen, E., Hopper, D.J., Back, J., 2009. Residual amplitude modulation mechanisms in modulation transfer spectroscopy that use electro-optic modulators. *Meas. Sci. Technol.*, **20**(2):1-8. [doi:10.1088/0957-0233/20/2/025 302]

Jin, Z., Zhang, G., Mao, H., *et al.*, 2012. Resonator micro optic gyro with double phase modulation technique using an FPGA-based digital processor. *Opt. Commun.*, **285**(5): 645-649. [doi:10.1016/j.opt-com.2011.11.017]

Lefevre, H., 1993. The Fiber-Optic Gyroscope. Artech House, London, United Kingdom, p.5-26.

Li, X., Ge, C., Zhang, C., 2009. The influence of residuary intensity modulation of Y waveguide on the performance of IFOG. *Opto-Electron. Eng.*, **36**(11):43-47 (in Chinese).

Ma, H., Jin, Z., Ding, C., *et al.*, 2003. Influence of spectral linewidth of laser on resonance characteristics in fiber ring resonator. *Chin. J. Lasers*, **30**(8):731-734 (in Chinese).

Ma, H., Jin, Z., Ding, C., *et al.*, 2004. Research on signal detection method of resonator fiber optical gyro. *Chin. J. Lasers*, **31**(8):1001-1005 (in Chinese).

Ma, H., Lu, X., Yao, L., *et al.*, 2012. Full investigation of the resonant frequency servo loop for resonator fiber-optic gyro. *Appl. Opt.*, **51**(21):5178-5185. [doi:10.1364/AO.51. 005178]

Malvern, A., 1992. Progress toward fiber optic gyro production. Fiber Optic Gyros: 15th Anniversary Conf. Int. Society for Optics and Photonics, p.48-64. [doi:10.1117/ 12.135035]

Meyer, R.E., Ezekiel, S., Stowe, D.W., *et al.*, 1983. Passive fiber-optic ring resonator for rotation sensing. *Opt. Lett.*, **8**(12):644-646. [doi:10.1364/OL.8.000644]

Sathian, J., Jaatinen, E., 2012. Intensity dependent residual amplitude modulation in electro-optic phase modulators. *Appl. Opt.*, **51**(16):3684-3691. [doi:10.1364/AO.51.00 3684]

Savatinova, I., Tonchev, S., Todorov, R., *et al.*, 1996. Electro-optic effect in proton exchanged $LiNbO_3$ and $LiTaO_3$ waveguides. *J. Lightw. Technol.*, **14**(3):403-409. [doi:10. 1109/50.485600]

Shupe, D.M., 1981. Fiber resonator gyroscope: sensitivity and thermal nonreciprocity. *Appl. Opt.*, **20**(2):286-289. [doi: 10.1364/AO.20.000286]

Wang, D., Sheng, F., 2007. Residuary intensity modulation of the phase modulator in IFOG and its measurement. *Opto-Electron. Eng.*, **34**(7):26-29 (in Chinese).

Wang, W., Zhang, G., 1995. The effect of residual intensity modulation of Ti: $LiNbO_3$ phase modulator in closed-loop FOG. *J. Chin. Inert. Technol.*, **3**(1):55-58 (in Chinese).

Ying, D., Ma, H., Jin, Z., 2008a. Resonator fiber optic gyro using the triangle wave phase modulation technique. *Opt. Commun.*, **281**(4):580-586. [doi:10.1016/j.optcom.2007. 10.012]

Ying, D., Ma, H., Jin, Z., 2008b. Dynamic characteristics of R-FOG based on the triangle wave phase modulation technique. *Opt. Commun.*, **281**(21):5340-5343. [doi:10. 1016/j.optcom.200807.042]

Ying, D., Demokan, M.S., Zhang, X., *et al.*, 2010. Analysis of Kerr effect in resonator fiber optic gyros with triangular wave phase modulation. *Appl. Opt.*, **49**(3):529-535. [doi: 10.1364/AO.49.000529]

Zhang, G., Wang, W., 1996. The effect of polarization crosstalk of Ti: $LiNbO_3$ phase modulator in closed-loop fiber-optic gyro. *Missil. Space Veh.*, **221**(3):20-25 (in Chinese).

Zhang, X., Ma, H., Ding, C., *et al.*, 2005. Analysis on phase modulation spectroscopy of resonator fiber optic gyro. *Chin. J. Lasers*, **32**(11):1529-1533 (in Chinese).

Zhang, X., Ma, H., Zhou, K., *et al.*, 2006a. Experiments in PM-spectroscopy resonator fiber optic gyro. *Chin. J. Sens. Actuat.*, **19**(3):800-803 (in Chinese).

Zhang, X., Ma, H., Ding, C., *et al.*, 2006b. Optical Kerr effect in phase modulation spectroscopy resonator fiber optic gyro. *Chin. J. Laser*s, **33**(6):814-818 (in Chinese).